U-Pb age, whole-rock geochemistry and radiogenic isotopic compositions of Late Cretaceous volcanic rocks in the central Aishihik Lake area, Yukon (NTS 115H)

G.A. Morris
Geological Survey of Sweden, Uppsala, Sweden

J.K. Mortensen[1]
University of British Columbia, Vancouver BC

S. Israel
Yukon Geological Survey, Whitehorse YT

Morris, G.A., Mortensen, J.K., and Israel, S., 2014. U-Pb age, whole-rock geochemistry and radiogenic isotopic compositions of Late Cretaceous volcanic rocks in the central Aishihik Lake area, Yukon (NTS 115H). *In:* Yukon Exploration and Geology 2013, K.E. MacFarlane, M.G. Nordling, and P.J. Sack (eds.), Yukon Geological Survey, p. 133-145.

ABSTRACT

Geochemical, isotopic and U-Pb dating studies of volcanic rocks of the Tlansanlin Formation in central Aishihik Lake map area (115H) show that these are Late Cretaceous (75.8 ± 0.4 Ma to 77.3 ± 1.3 Ma), relatively primitive magmas that were emplaced in a continental arc setting. Intrusive rocks in the immediate area, associated with the Hopper porphyry and skarn and Sato porphyry occurrences (Yukon MINFILE 115H 019, 021, respectively), are similar in age and composition to the Tlansanlin Formation rock units, confirming the presence of a significant Late Cretaceous igneous and mineralizing event in the area. Significant porphyry and skarn occurrences associated with the Late Cretaceous intrusions in the Aishihik Lake area, as well as the important mineral deposits and occurrences associated with this magmatic event in the Dawson Range to the northeast (*e.g.*, Casino, Revenue-Nucleus, Sonora Gulch), underscore the metallogenic potential of this previously poorly recognized magmatic event.

[1] *jmortensen@eos.ubc.ca*

INTRODUCTION

At least seven separate suites of volcanic rocks of Late Cretaceous to Paleocene age have been recognized northeast of the Denali fault system in southwestern Yukon (Fig. 1). The Bennett Lake and Mount Skukum volcanic complexes in the southwestern Whitehorse map area (Morris and Creaser, 2003) and the Rhyolite Creek volcanoplutonic complex in the northwestern Aishihik Lake map area (Fig. 1; Israel *et al.*, 2011a,b; Israel and Westberg, 2011, 2012) have given Paleocene to Eocene emplacement ages. The Sifton Range volcanic complex in the eastern Aishihik Lake map area (Fig. 1) is undated but is also inferred to be Paleocene in age by Miskovic and Francis (2004) based on the age of Paleocene intrusive rocks that crosscut the complex. The Donjek Volcanics in the central Stevenson Ridge map area (Fig. 1; Templeman-Kluit, 1974; Murphy, 2007) have yielded preliminary Late Cretaceous crystallization ages (D. Murphy and J.K. Mortensen, unpublished data). The small Mount Creedon volcanic complex on the western side of Aishihik Lake in central Aishihik Lake map area (Fig. 1) is undated but has been inferred to be of Paleocene age in most recent map compilations (Johnston and Timmerman, 1997a; Israel *et al.*, 2011a). Finally, volcanic units immediately east of Aishihik Lake in the central part of the Aishihik Lake map area (Fig. 1) were previously assigned to the Carmacks Group (Tempelman-Kluit, 1974) and subsequently to a newly named Tlansanlin Formation with an assumed Late Cretaceous age by Johnston and Timmerman (1997b).

In this study we present previously unpublished major, trace and rare earth element data, as well as measured Nd and Sr isotopic compositions and two U-Pb zircon ages, for a suite of samples from the Tlansanlin Formation in the central Aishihik Lake area. We then use these results to better constrain the nature and timing of magmatism and discuss metallogenic implications for this part of southwestern Yukon.

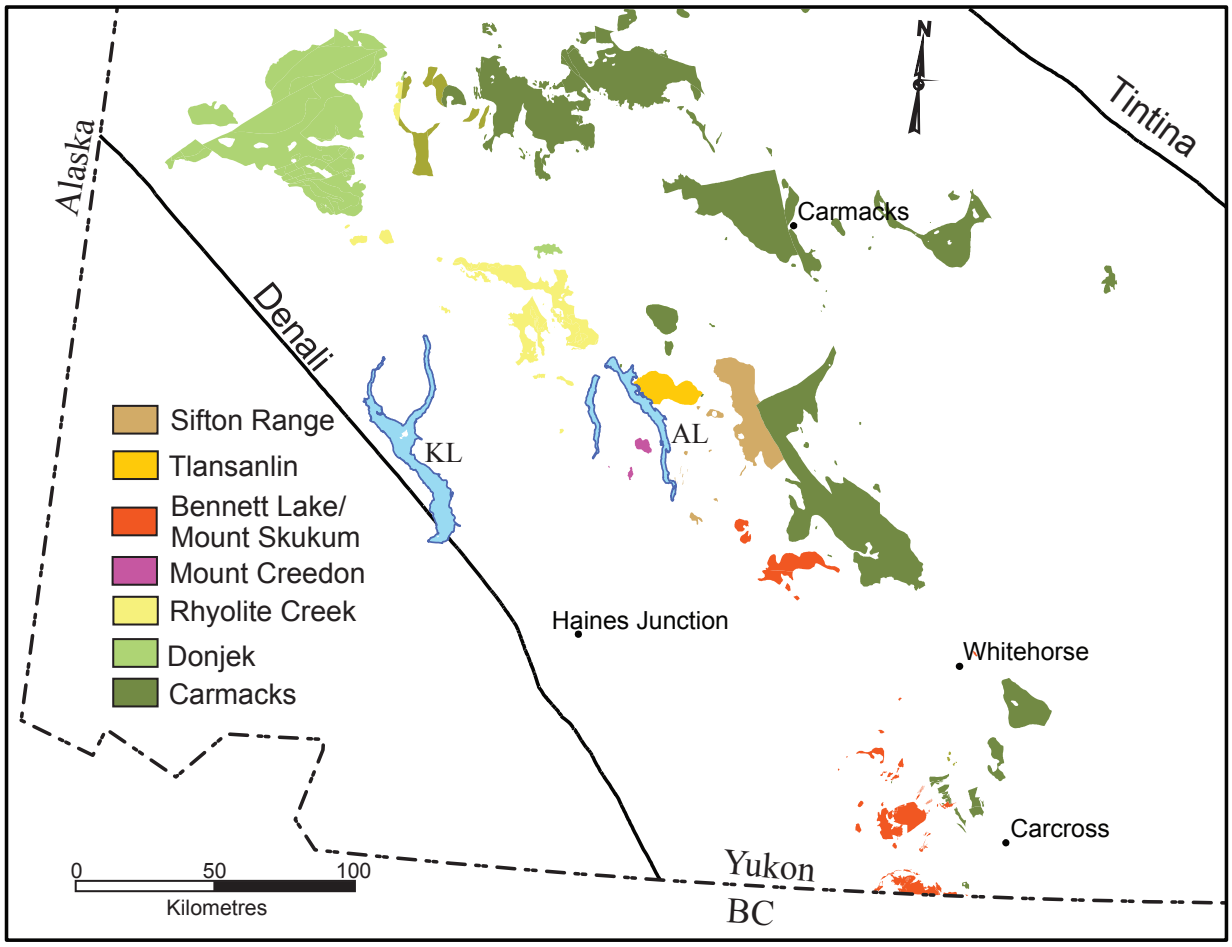

Figure 1. *Map showing the locations of the various Paleocene/Eocene and Late Cretaceous volcanic and plutonic assemblages in southwestern Yukon. Geology from Colpron (2013). AL = Aishihik Lake, KL = Kluane Lake.*

REGIONAL GEOLOGY OF THE AISHIHIK LAKE AREA

A simplified version of the geology of the Aishihik Lake map area is shown in Figure 2.

Metamorphic rocks assigned to the Yukon-Tanana Terrane (Snowcap and Finlayson assemblages; Israel *et al.*, 2011b) occur within a northwest-trending belt across the centre of the map area (Fig. 2). These rocks comprise metasedimentary and metavolcanic rocks, including quartz-muscovite ± garnet schist, carbonaceous biotite ± garnet schist and quartzite, garnet amphibolite and marble, as well as rare intermediate composition metaplutonic rocks. The metasedimentary units are undated in this area, but are assumed to be Mississippian and older based on correlations with well-dated rock units elsewhere in Yukon. Samples of granitic orthogneiss and possible metavolcanic units in the immediate vicinity of Aishihik Lake have given U-Pb crystallization ages of 352-344 Ma (Johnston *et al.*, 1996).

Plutonic rocks underlie much of the Aishihik Lake map area (Fig. 2). These include intermediate to felsic intrusions of the Early Jurassic Aishihik and Long Lake plutonic suites (Johnston *et al.*, 1996), which underlie large portions of the eastern half of the map area, together with felsic intrusive rocks of the mainly Paleocene Ruby Range batholith, which forms a northwest-trending belt across the southern and western part of the map area (*e.g.*, Israel *et al.*, 2011a; Israel and Westberg, 2011; Fig. 2). Numerous smaller intrusions that crosscut the Early Jurassic intrusions and their metamorphic wall rocks northeast of the Ruby Range batholith have in the past been mainly assumed to be related to the batholith itself. Several of these intrusions, however, have yielded Late Cretaceous crystallization ages. A small body of hornblende diorite that hosts the Sato porphyry copper occurrence (Yukon MINFILE 115H 021; Fig. 2) yielded two conventional U-Pb zircon ages of 78.2 ± 0.1 Ma and 78.8 ± 0.2 Ma (Lewis and Mortensen, 1998). Another small stock immediately east of Hopkins Lake (the "Hopper intrusion"; Johnston and Timmerman, 1997b; Blumenthal, 2010) gave U-Pb zircon ages by laser ablation ICP-MS methods at 77.2 ± 1.2 Ma and 76.0 ± 1.1 Ma (Blumenthal, 2010; a third sample gave a calculated age of 83.7 ± 1.9 Ma; however, the analytical data from this sample shows a high degree of scatter and the significance of the calculated age is uncertain). Johnston and Timmerman (1997b) describe scattered outcrops of volcanic rocks in the northeastern part of the Hopkins Lake map area (115H/7) as comprising "heterogeneous grey, green and maroon, poorly consolidated, intermediate to felsic, feldspar and hornblende-feldspar porphyritic tuff, flow breccia and volcaniclastic rocks". These volcanic units overlie a package of conglomerate, sandstone and mudstone that contains a large proportion of reworked volcanic rocks as well as minor tuff. Collectively these two units are called the Tlansanlin Formation (Johnston and Timmerman, 1997b), named for a type locality along the Tlansanlin Creek on the east side of Aishihik Lake (Fig. 2). In the vicinity of the Sato occurrence, in the northeastern Hopkins Lake map area, the upper Tlansanlin Formation volcanic rocks are interpreted to unconformably overlie Early Jurassic Long Lake suite intrusive rocks, but to be crosscut by the ~78 Ma diorite body that hosts the Sato porphyry-style mineralization. This interpreted relationship implies a probable Late Cretaceous age for the Tlansanlin Formation volcanic rocks (Johnston and Timmerman, 1997b).

Intermediate to felsic volcanic rocks interlayered with volcaniclastic units underlies part of the northeastern Hopkins Lake map sheet and areas farther to the north and east (Fig. 2). Although Johnston and Timmerman (1997b) included these units in their Tlansanlin Formation, Miskovic and Francis (2004) include them in the Sifton Range complex.

Johnston and Timmerman (1997b) also included a number of narrow, north-south trending, fine grained mafic dikes that are widespread in the Hopkins Lake map area (115H/7) as part of the Late Cretaceous magmatic suite. None of these dikes have been dated thus far. North-south trending quartz-feldspar porphyry dikes are also widespread in the southern Hopkins Lake and adjacent Aishihik Lake map areas; these dikes are also undated but are inferred by Johnston and Timmerman (1997a) and Israel *et al.* (2011a) to be Paleocene or Eocene in age.

TLANSANLIN FORMATION VOLCANIC UNITS IN THE CENTRAL AISHIHIK LAKE AREA

Volcanic rock units that comprise the upper part of the Tlansanlin Formation of Johnston and Timmerman (1997b) underlie an area of approximately 200 km^2 to the east of Aishihik Lake (Fig. 2). The volcanic sequence consists of extensive, flat-lying basalt, basaltic andesite, andesite and dacite lava flows, lapilli and welded pyroclastic flows. Basalt and basaltic andesite are generally fine-grained with

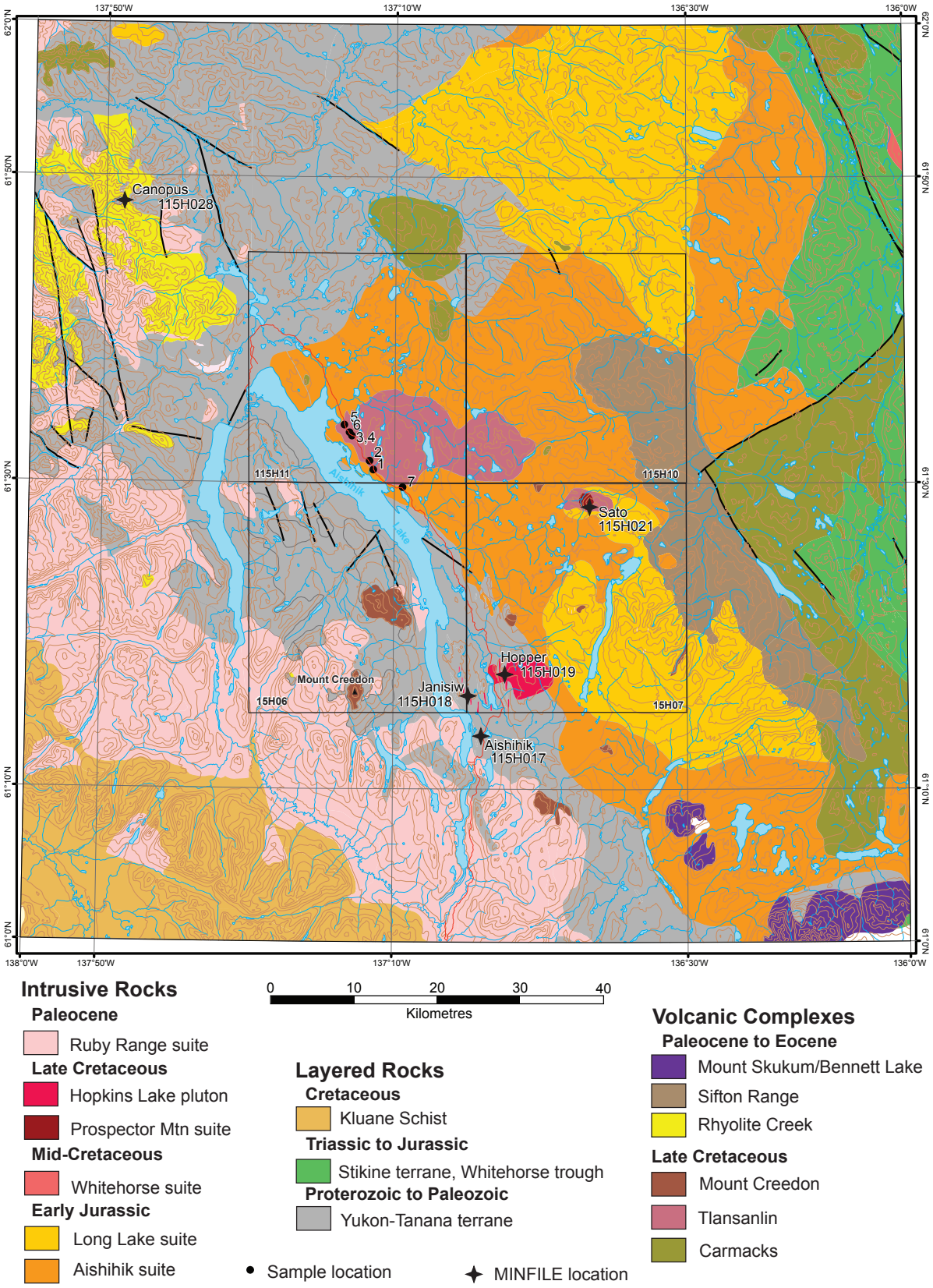

***Figure 2**. Simplified geology of the Aishihik Lake map area. Sample location numbers correspond to those in Table 1. Geology is modified from Johnston and Timmerman (1997a,b), Israel and Westberg (2011), and Israel et al. (2011a).*

microphenocrysts of olivine and pyroxene in a groundmass dominated by calcic plagioclase. Andesite and dacite contain phenocrysts of plagioclase, hornblende and, rarely, pyroxene up to 5 mm in size, in a fine-grained to devitrified glass matrix. Plagioclase phenocrysts commonly display fine scale cyclic zoning and are generally broken. Mafic phenocryst phases commonly show reaction rims of oxide minerals.

Volcanic rocks in the study area were originally mapped by Cockfield (1927) as "Jurassic (?) to Triassic (?) older volcanics" but were subsequently mapped by Templeman-Kluit (1974) as the "varicoloured acid tuff." They were later incorporated into the Mount Creedon Volcanic Suite of Johnston and Timmerman (1994), which were thought to correlate with the Mount Nansen Group and/or the Carmacks Group, as defined farther to the northeast in the Dawson Range. More recent geochronological studies have shown that the Mount Nansen and Carmacks groups are middle and Late Cretaceous in age, respectively (Allan *et al*., 2013, and references therein). Johnston and Timmerman (1997b) subsequently included the volcanic rocks into their Tlansanlin Formation, tentatively assigned to the Late Cretaceous. Due to the flat lying and undeformed nature of lava flows, they were, however, thought to have been erupted following uplift of the Palaeocene-Eocene Ruby Range batholith and the associated Aishihik and Kluane metamorphic assemblages. The earliest date for this uplift has been put at ~55 Ma (Erdmer and Mortensen, 1993). Clasts that were thought to have been derived from the Ruby Range batholith have also been identified within the volcanic strata at Aishihik Lake (Johnson and Timmerman, 1994). This evidence suggested a Paleocene or Eocene age rather than an association with any Cretaceous magmatic event, including the Carmacks Group volcanics (which in any case do not generally contain dacite) or the Mount Nansen volcanics (Morris and Creaser, 1998).

SAMPLE DESCRIPTIONS

Whole-rock geochemistry, together with Sr and Nd isotopic compositions and U-Pb zircon age, were determined for a suite of six samples of massive dikes and volcanic flows and domes of the Tlansanlin Formation that were collected during a reconnaissance level investigation of this sequence by the first author. Sample locations and brief descriptions are given in Table 1.

Sample GM97 A94 was collected from a partially weathered and well fractured dike and is basaltic or trachybasaltic in composition (see below). Sample GM97 A95 is an andesite collected from a poor exposure of what is thought to be a dike, and is also moderately weathered. Sample GM97 A96 is a basaltic andesite, also from a moderately weathered and poorly exposed dike whereas sample GM97 A97 is a much less weathered basaltic andesite collected from a sub-aerial flow with well-developed columnar joints. Sample GM97 A98 is a dacite which shows two well mixed but distinct components, probably as a result of magma mingling. In outcrop it was unclear if this was a small high-level intrusion or a sub-aerial dome. Sample GM97 A99 is also dacitic, appears unaltered and was clearly emplaced as a flow. Both dacite samples contain numerous feldspar phenocrysts (30-40%).

Table 1. *Locations and field-based lithological descriptions of Tlansanlin Formation igneous rocks in the central Aishihik Lake map area.*

Sample	Number on Fig. 2	Lithological Description	Latitude	Longitude	UTM (NAD83)		
					Zone	Northing	Easting
GM 97 A94	1	Fractured and variably weathered basaltic dike	61 30′53.4″	137 12′52.6″	8V	6822135	382180
GM 97 A95	2	Moderately weathered andesite dike(?)	61 31′28.9″	137 13′32.5″	8V	6823253	381629
GM 97 A96	3	Moderately weathered basaltic andesite dike	61 33′07.5″	137 15′50.3″	8V	6826373	379699
GM 97 A96R	4	Moderately weathered basaltic andesite dike	61 33′07.5″	137 15′50.3″	8V	6826373	379699
GM 97 A97	5	Fine-grained basaltic andesite flow with well-developed columnar joints	61 33′52.0″	137 16′57.2″	8V	6827784	378760
GM 97 A98	6	Highly weathered plagioclase-phyric dacite intrusion or dome	61 33′20.9″	137 16′16″	8V	6826802	379334
GM 97 A99	7	Massive unaltered plagioclase-phyric dacite flow	61 29′43.5″	137 09′05.5″	8V	6819862	385464

WHOLE-ROCK GEOCHEMISTRY AND RADIOGENIC ISOTOPES

ANALYTICAL METHODS

Major and trace elements were analysed by X-ray fluorescence (XRF) spectrometry at Washington State University's Peter Hooper Geoanalytical Laboratory in Pullman, Washington, USA. (Table 2). Analytical procedures, accuracy, and precision for data are reported in Johnson *et al*. (1999). Rare-earth elements (REE) and selected trace elements were also analysed by inductively coupled plasma – mass spectrometry (ICP–MS) (Table 3) at the Peter Hooper Geoanalytical Laboratory following procedures given in Knaack *et al*. (1994). Of the trace elements analysed, Ba, Rb, Sr, Th, Nb, Y, Pb, La, Ce, and Sc duplicate the XRF analysis to provide a certain degree of internal monitoring. Of these, the Ba, Sr, Th, Nb, Sc, and Pb values by ICP–MS are preferred, particularly at lower abundances, whereas the XRF values for Rb and Y are considered more precise (Knaack *et al*. 1994; Johnson *et al*. 1999). For the REE, La and Ce are also duplicated and the ICP–MS data are preferred, particularly at the low abundances observed here.

Table 2. *Major and selected trace element data by X-ray Fluorescence. Major element data is presented as weight percent oxide normalised to 100%.*

Sample	GM97 A94	GM97 A95	GM97 A96	GM97 A97	GM97 A98	GM97 A99	GM 97A96	GM97 A96R
Major Elements. normalized (wt%)								
SiO_2	52.6	62.42	55.47	56.25	67.4	65.24	55.47	55.47
Al_2O_3	18.15	17.07	17.46	16.37	15.83	16.72	17.46	17.41
TiO_2	1.12	0.87	1.05	0.93	0.61	0.5	1.05	1.04
FeO*	7.15	5.41	7.54	7.01	4.5	3.56	7.54	7.65
MnO	0.14	0.1	0.14	0.13	0.04	0.09	0.14	0.14
CaO	10.19	6.88	10.66	7.94	2.73	5.24	10.66	10.67
MgO	4.57	2.39	2.89	6.12	0.72	2.18	2.89	2.91
K_2O	1.9	1.42	1.29	1.12	1.93	1.36	1.29	1.29
Na_2O	3.7	3.14	3.14	3.81	5.96	4.96	3.14	3.06
P_2O_5	0.48	0.3	0.36	0.32	0.28	0.15	0.36	0.36
Original total	94.62	96.35	94.21	97.9	99.66	98.56	94.21	94.22
Trace Elements (ppm)								
Ni	93	26	69	98	16	22	69	68
Cr	241	123	255	281	50	69	255	255
Sc	27	16	25	25	9	11	25	25
V	190	135	168	159	100	74	168	168
Ba	1195	1342	945	1965	1034	1709	945	922
Rb	40	28	14	25	39	17	14	13
Sr	763	743	663	775	480	573	663	664
Zr	152	156	142	139	136	120	142	141
Y	22	18	18	18	14	15	18	19
Nb	21	9	10	10	8	6	10	10
Ga	19	18	19	15	14	18	19	19
Cu	27	25	30	38	15	10	30	28
Zn	89	77	115	81	42	59	115	107
Pb	3	4	5	8	15	10	5	6
La	42	18	21	23	25	11	21	21
Ce	71	49	31	40	31	25	31	56
Th	9	6	3	3	7	4	3	1

***Table 3**. Rare earth and selected trace element data by ICP-MS (in ppm).*

Sample	GM 97 A97	GM 97 A98	GM 97 A99
La	21.66	25.08	14.73
Ce	41.63	41.7	26.37
Pr	4.89	4.49	3.03
Nd	21.08	17.69	12.26
Sm	4.78	3.61	2.95
Eu	1.56	1.12	1.05
Gd	4.55	3.29	3.03
Tb	0.66	0.49	0.45
Dy	3.73	2.72	2.63
Ho	0.73	0.51	0.54
Er	1.9	1.4	1.45
Tm	0.27	0.2	0.21
Yb	1.61	1.23	1.33
Lu	0.27	0.2	0.21
Ba	1918	870	1616
Th	4.16	7.99	4.45
Nb	10.01	7.35	5.2
Y	20.08	14.71	15.51
Hf	3.1	3.03	2.7
Ta	0.59	0.55	0.39
U	1.39	2.79	1.72
Pb	7.44	16.71	12.08
Rb	23.7	30.1	17.4
Cs	8.55	0.54	0.28
Sr	772	432	543
Sc	26.3	12.2	12.8

Three samples were analysed for Rb–Sr and Sm–Nd isotopes at the Radiogenic Isotope Facility of the University of Alberta, Edmonton, Alberta (Table 4). Samples were totally spiked and dissolved in a 10:2 mix of concentrated HF:concentrated HNO_3 acid at approximately 120°C for 5 days. Samples were then converted to chloride salts using concentrated HCl. Rb, Sr, and the REE were separated from the whole sample by passing through standard cation exchange columns. Rb and Sr separates were passed through a second ion exchange column before isotopic analysis. Sm and Nd were separated from the other REE by being passed through HDEHP-coated (Di(2-ethylexyl) orthophosphoric acid coated) BioBead columns, then analysed isotopically. Rb and Sm samples were analysed on a VG Micromass 30 single- collector mass spectrometer. Sr and Nd were analysed on a VG Micromass 354 fully automated 5-collector mass spectrometer. Rb and Sr data were standardised to NBS-987, while Sm and Nd data were standardised to an internal standard, then corrected to the La Jolla standard. During the period of these analyses, an average $^{87}Sr/^{86}Sr$ ratio of 0.710213 (1SD (standard deviation) = 0.000032, n = 22) was recorded for NBS 987. To facilitate comparisons with other laboratories, a correction factor of +0.000032 was applied to all data that are reported relative to an NBS 987 ratio of 0.710245. Likewise a $^{143}Nd/^{144}Nd$ ratio of 0.511839 (1SD = 0.000011, n = 4 determinations) was recorded for the La Jolla standard. A correction factor of 0.000011 was added to all analyses that are reported relative to an expected value for La Jolla of 0.511850. An age of 76 Ma was used to calculate Sr_i (initial Sr ratio) and Nd_i (initial Nd ratio).

RESULTS

Major and trace element compositions for six samples (together with one replicate analysis) are shown in Table 2, and additional high field strength (HFS) and rare earth elements (REE) for three of the samples are shown in Table 3. The analyses are plotted on a variety of petrological discriminant diagrams in Figure 3, and tectonic discriminant diagrams and spider diagrams depicting ratios of HFSE and REE compositions to average values for primitive mantle and chondrites in Figure 4. Fields for whole rock compositions from the variably altered diorite and quartz monzonite that hosts the Sato Cu-Mo porphyry occurrence (from Lewis, 1997), and

***Table 4**. Results of Rb Sr and Sm Nd isotopic analyses. Analysed data corrected to an expected value of 0.710213 for NBS 987 (Rb Sr) and 0,511839 for the La Jolla standard (Sm Nd). Initial ratios calculated assuming an age of 76 Ma based upon data presented in this paper.*

2σ error	$Sr_{i(76Ma)}$	Sm ppm	Nd ppm	$^{147}Sm/^{144}Nd$	$^{143}Nd/^{144}Nd$	$^{143}Nd/^{144}Nd$ corrected	2σ error	$Nd_{i(76Ma)}$	εNd_{76}
0.00001	**0.705**	4.46	21.91	0.1241	0.512678	0.512689	0.000009	0.512627	**1.7**
0.00001	**0.70531**	3.56	19.19	0.1127	0.512678	0.512689	0.000008	0.512633	**1.8**
0.00002	**0.70563**	2.73	12.99	0.1278	0.512607	0.512618	0.000009	0.512574	**0.1**

altered and unaltered granodiorite of the Hopper intrusion on the east side of Hopkins Lake (Fig. 2) are shown for reference where this information is available.

Particular note should be made of the low totals obtained from the more basic dikes that were analysed in this study. This, combined with the generally altered appearance of some of the sampled outcrops, suggests that significant alteration of samples has taken place. Classification and tectonic discrimination diagrams that rely on the more mobile elements should therefore be treated with caution.

Samples range in silica content from 52.6 to 67.4 wt% SiO_2. The sample suite plots as calcic, according to the classification of Peacock (1931), or calc-alkaline according to Peccerillo and Taylor (1976; Fig. 3b). On plots of total alkalis vs. SiO_2 and K_2O vs. SiO_2 (Le Bas *et al.*, 1986, and Peccerillo and Taylor, 1976 respectively; Figs. 3a,b) all but one of the samples plot as subalkaline (Fig. 3b), and range in composition from basaltic andesite to dacite/trachydacite. On immobile element ratio plots such as Zr/TiO_2 vs Nb/Y (Winchester and Floyd, 1977; Fig. 3c), however, the analyses show much less scatter, falling mainly in the basalt and basaltic andesite fields. This suggests that at least some of the observed range of SiO_2 contents, and potentially also the alkali-metals contents, may be a result of element mobility related to hydrothermal alteration or surface weathering.

Incompatible trace element concentrations for the sample suite (Tables 2 and 3) are comparable to similar rock types in present day subduction related volcanic arcs (Ni >90 ppm in basalt and basaltic andesite to ~20 ppm in dacite (*e.g.*, Bacon *et al.*, 1997). Most incompatible trace element concentrations (*e.g.*, Ba, Rb, Zr and Y) are relatively low although there is a somewhat higher concentration of Sr at equivalent silica contents compared with arc volcanic rocks. All rocks analysed show the distinctive decoupling of HFS and large ion lithophile (LIL) elements associated with arc magmatism, or reactivation of such rocks. There is a slight decrease in the concentrations of REEs with increasing silica, particularly evident in the heavy REEs, but there is a negligible Eu anomaly, even at the highest silica values suggesting that the fractionation of plagioclase was not a key factor in the evolution of this suite.

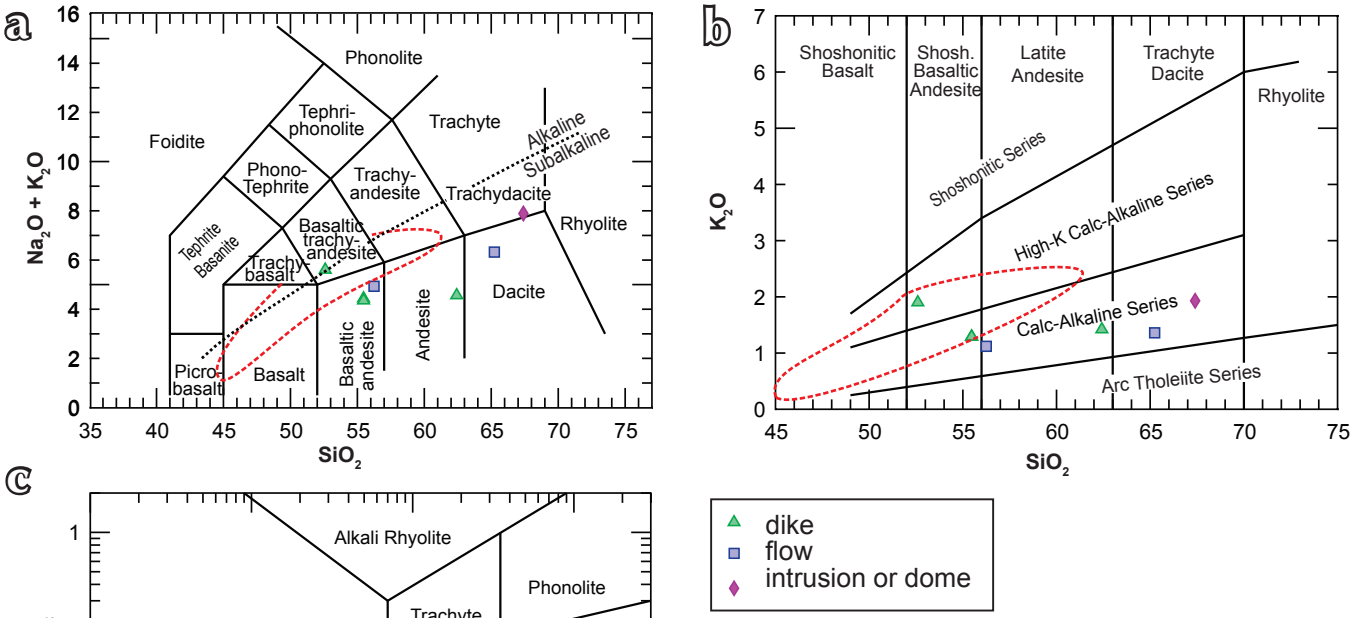

***Figure 3**. Plots of whole rock geochemical analyses of volcanic and intrusive rocks from the study area: (a)total alkalis vs. SiO_2 plot from Le Bas et al. (1986); fields for subalkaline vs. alkaline compositions from Irvine and Baragar (1971); (b) K_2O vs. SiO_2 from Pecarrillo and Taylor (1976); (c) immobile element ratio plot from Winchester and Floyd (1977) as revised by Pearce et al. (1996). Red dashed field shows the range of compositions for altered and unaltered intrusive rocks that host the Sato porphyry Cu-Mo occurrence (115 H/7) (data from Lewis, 1997).*

Extended plots of HFSE and REE ratios to model primitive mantle (Sun and McDonough, 1989; Fig. 4a) show Nb and Ti depletions typical of subduction-related magmatism. On a tectonic discriminant plot of Y+Nb vs. Rb (Pearce *et al.*, 1986; Fig. 4c) all of the samples fall well within the "volcanic arc" field (although it is possible that there may have been some post-crystallization mobility of Rb; see above discussion). One basaltic andesite sample returns a Sr_i ratio of 0.70500 and an ε_{Ndi} value of +1.7 whereas dacite from the same area return Sr_i ratios of 0.70531 to 0.70563 and ε_{Ndi} of +1.8 to +0.1 (Table 4). Such values are typical for fairly young and primitive continental arc rocks.

Taken together, the measured whole rock geochemical and isotopic compositions of the sample suite are typical of continental arc volcanic rocks. The slightly elevated K and lower compatible element concentrations at the basaltic end of the range when compared to typical arc volcanic rocks from the Cascade Range (Bacon *et al.*, 1997) could be attributed to the observed alteration and weathering of these rocks, but nothing that could not be argued to be the result of assimilation and fractional crystallization (AFC) processes, possibly together with minor crustal contamination in a continental arc setting. The fairly primitive isotopic values argue against remobilisation or significant assimilation of older continental crust.

U-PB AGE DETERMINATIONS

ANALYTICAL METHODS

U-Pb dating of two samples of dacite from the sample suite was carried out using isotopic dilution-thermal ionization mass spectrometry (ID-TIMS) methods. Zircons were separated from ~3 kg samples using conventional crushing, grinding, wet shaking table, heavy liquids and magnetic methods. U-Pb ID-TIMS analyses were carried out at the Pacific Centre for Isotopic and Geochemical Research at the University of British Columbia, using methods as described by Mortensen *et al.* (2008). Multigrain zircon samples were analysed, and all of the zircons were strongly air-abraded prior to analysis in an attempt to minimize the effects of post-crystallization Pb-loss. Errors on calculated ages are given at the 2σ level (95% confidence interval).

RESULTS

Zircons recovered from the two samples consisted of euhedral, clear, colorless, stubby to elongate, euhedral prismatic grains containing rare clear colorless inclusions, and exhibiting vague concentric growth zoning but no obvious inherited cores. Four multigrain fractions were analysed from each sample. Results are listed in Table 5 and are plotted on conventional concordia diagrams in Figure 5.

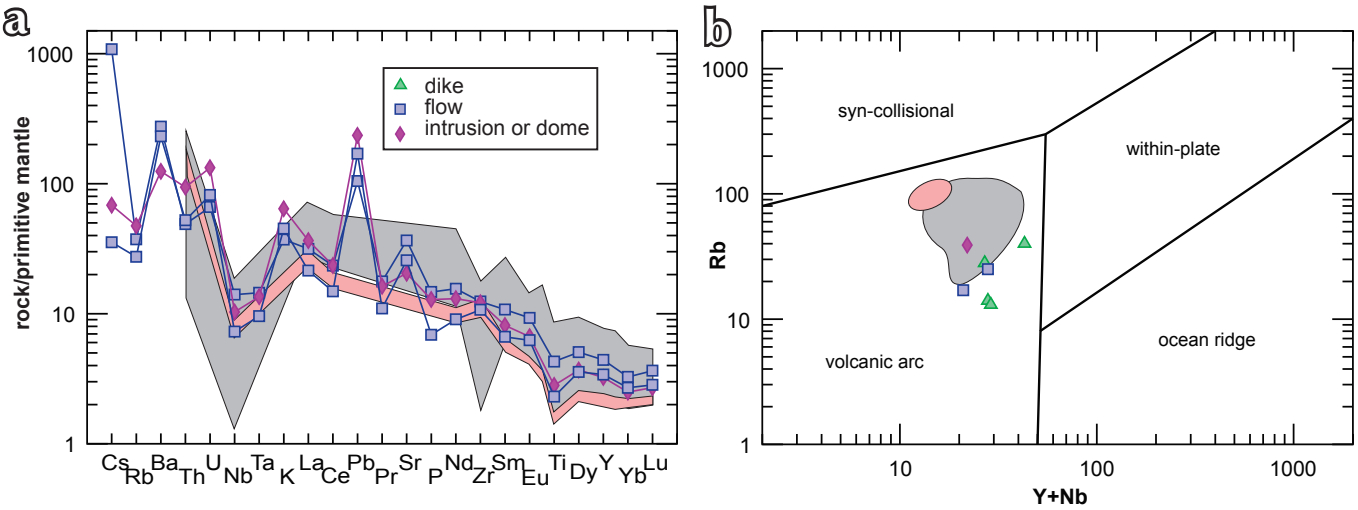

***Figure 4**. (a) extended plot of HFSE and REE ratios of Tlansanlin Formation volcanic and intrusive rocks from this study to model primitive mantle values (from Sun and McDonough, 1989); (b) tectonic discriminant plot for Tlansanlin Formation volcanic and intrusive rocks (from Pearce et al., 1984). Shaded fields in (a) is for altered and unaltered granodiorites from the Hopper intrusion (grey), and quartz-feldspar porphyry dike cutting the Hopper intrusion (pink), from Blumenthal (2010).*

***Table 5**. U-Pb isotopic analyses of zircons from two Tlansanlin Formation dacite samples from the central Aishihik Lake map area.*

Sample	Wt	U	Pb[2]	$^{206}Pb/^{204}Pb$	total common	%	$^{207}Pb/^{235}U$[4]	(±% 1σ)	$^{206}Pb/^{238}U$[4]	(±% 1σ)	Rho	$^{207}Pb/^{206}Pb$[4]	(±% 1σ)	$^{206}Pb/^{238}U$ age	(±2σ)	$^{207}Pb/^{235}U$ age	(±2σ)	$^{207}Pb/^{206}Pb$ age	(±2σ)
Description[1]	(mg)	(ppm)	(ppm)	(meas.)[3]	Pb (pg)	^{208}Pb[2]								Ma		Ma		Ma	
97GM A98 (dacite intrusion or dome)																			
A: N10,+134	0.06	461	5.8	449	46	14.6	0.0778	1.3	0.01182	0.12	0.52	0.04784	1.24	75.8	0.2	76.2	1.9	91.6	58.1
B: N10,+134	0.055	365	4.6	369	41	15.2	0.07777	0.74	0.01176	0.21	0.67	0.04796	0.63	75.4	0.3	76.1	1.1	97.1	29.5
C: N10,+134	0.056	440	5.4	1866	10	13.3	0.0781	0.2	0.01186	0.08	0.46	0.04777	0.18	76	0.1	76.4	0.3	87.7	8.5
D: N10,+134	0.057	428	5.3	1669	11	14.2	0.07766	0.21	0.01181	0.09	0.39	0.04769	0.19	75.7	0.1	75.9	0.3	84.1	9.2
97 GM A99 (dacite flow)																			
A: N10,+134	0.056	411	5.1	350	55	7.4	0.08524	0.67	0.01279	0.31	0.50	0.04835	0.58	81.9	0.5	83.1	1.1	116.5	27.1
B: N10,+134	0.041	331	3.9	207	54	8	0.07976	1.24	0.01208	0.32	0.67	0.04789	1.05	77.4	0.5	77.9	1.9	93.6	49.5
C: N10,+134	0.049	476	5.6	279	66	9	0.07799	0.88	0.01194	0.25	0.67	0.04738	0.73	76.5	0.4	76.3	1.3	68.4	34.8
D: N10,+134	0.047	466	5.5	313	56	7.6	0.07962	0.68	0.01213	0.2	0.66	0.0476	0.56	77.7	0.3	77.8	1	79.5	26.7

1 N10 = non-magnetic at 10 degrees side slope on Frantz magnetic separator; grain size given in microns

2 radiogenic Pb; corrected for blank, initial common Pb, and spike

3 corrected for spike and fractionation

4 corrected for blank Pb and U, and common Pb

Four fractions of zircon were analysed from each of the two samples. Four analyses for sample GM97 A98 (dacite intrusion or dome) fall on or near concordia, with some scatter. A weighted average of the $^{206}Pb/^{238}U$ ages for three of the analyses gives 75.8±0.4 Ma, which is interpreted to be the best estimate for the crystallization age of the sample. A fourth zircon fraction yields a slightly younger $^{206}Pb/^{238}U$ age, probably reflecting minor post-crystallization Pb-loss that was not completely eliminated by the air abrasion.

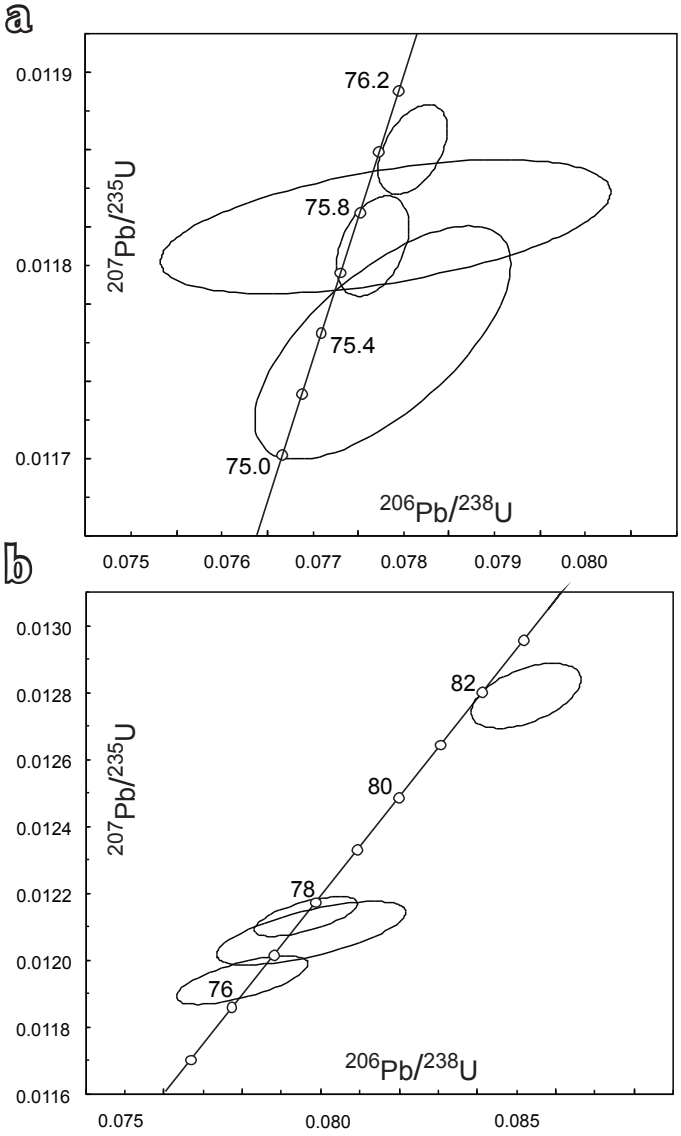

***Figure 5**. Conventional U-Pb concordia plot for zircons from the Tlansanlin Formation volcanics: (a) sample GAM97-A98 (dacite intrusion or dome); (b) sample 97GAM-A99 (dacite flow).*

Four analyses from sample GM97 A99 (dacite flow) also scatter along concordia. One analysis gives a distinctly older $^{206}Pb/^{238}U$ age than the others (81.2 Ma) and is interpreted to have contained an older zircon component, probably as one or more somewhat older xenocrysts that were entrained from underlying rock units. The other three analyses give $^{206}Pb/^{238}U$ ages in the range of 76.5±0.4 Ma to 77.7±0.3 Ma (Table 3, Fig. 5b). The two older of these give a weighted average $^{206}Pb/^{238}U$ age of 77.3±1.3 Ma, which gives the best estimate of the crystallization age of the sample. The fourth zircon fraction has likely suffered very minor post-crystallization Pb-loss.

DISCUSSION

Johnston and Timmerman (1997b) report crosscutting relationships which indicate that plutons at the Sato porphyry occurrence (78.2±0.1 Ma and 78.8±0.2 Ma; Lewis and Mortensen, 1998) intrude Tlansanlin Formation volcanic rocks in the northern Hopkins Lake area. Taken together with ages of 75.8±0.4 Ma and 77.3±1.3 Ma reported here for a dacite flow and an associated flow or dome, respectively, from within the Tlansanlin Formation suggests an age range of at least 3 m.y. for Tlansanlin magmatism in this area. Ages of 77.2±1.2 Ma and 76.0±1.1 Ma reported by Blumenthal (2010) for two samples of the Hopper intrusion in the southwestern Hopkins Lake map area indicate that this intrusion is likely also part of this same magmatic event.

Major element geochemical compositions from the Sato and Hopper intrusions (Lewis and Mortensen, 1998; Blumenthal, 2010) indicate that these bodies are also calc-alkaline and generally overlap with our measured compositions for volcanic rocks in the Tlansanlin Creek area (Figs. 3a,b). HFSE and REE compositions from the Hopper intrusion (fields from Blumenthal, 2010) are also very similar to the Tlansanlin Formation volcanic rocks (Figs. 4a,b). It is interesting to note that two samples of undated, north-south trending quartz-feldspar dikes that cut the Hopper intrusion give compositions (including HFSE and REE; Blumenthal, 2010; Figs. 4a,b) that are also very similar to the Tlansanlin Formation volcanic rocks. These dikes are typical of a suite of north-south trending quartz-feldspar dikes that area widespread throughout the central and western Aishihik Lake map area, and have been interpreted by previous workers to be Paleocene or Eocene in age (Johnston and Timmerman, 1997a,b; Israel *et al.*, 2011a; Israel and Westberg, 2012). Blumenthal's (2010) data indicates that the porphyry dikes were derived by similar igneous processes as the Late Cretaceous magmatism, and also suggest that some or all of the porphyry dikes may actually be Late Cretaceous in age rather than Paleocene or Eocene. The Late Cretaceous magmatism may be considerably more widespread than previously thought, and possibly includes the presently undated Mount Creedon and Sifton Range volcanic complexes, as well as some of the volcanic and intrusive rocks presently mapped as the Paleocene or Eocene Rhyolite Creek volcanic complex farther to the west, as well as some phases of the Ruby Range batholith and associated dikes in that area.

Recent regional studies throughout the Dawson Range have led to the recognition of two distinct pulses of Late Cretaceous magmatism in this region (Allan *et al.*, 2013). An early phase of magmatism ("early Late Cretaceous"; 79-71 Ma) is represented by relatively small volume intrusions that form a belt along the trend of the Dawson Range, and yield compositions that are consistent with having formed in a continental magmatic arc. A slightly later magmatic event ("late Late Cretaceous"; 72-67 Ma) includes both small intrusions as well as the aerially extensive volcanic rocks of the Carmacks Group. This younger phase of magmatism is present throughout the Dawson Range but also extends far to the northeast, and reflects magmatic processes that are not thought to be directly subduction-related (Allan *et al.*, 2013). Although a significant number of porphyry, vein and other styles of mineralization have been shown to be related to the "late Late Cretaceous" magmatism, the "early Late Cretaceous" event appears to host larger and economically more important mineral deposits (*e.g.*, Casino, Revenue/Nucleus, Cyprus). The recognition of the potentially widespread occurrence of "early Late Cretaceous" volcanic rocks and high level intrusions in the central Aishihik Lake area therefore considerably enhances the mineral deposit potential of that region. Several porphyry Cu-Mo occurrences are already known in the area (*e.g.*, Sato - 115H 021, and Hopper - 115H 019), as well as Cu and Cu-Mo-W skarns (*e.g.*, Hopkins - 115H 019, and Janisiw - 115H 018) (Fig. 2). Israel *et al.* (2011b) and Israel and Westberg (2012) noted that the observed transition from high level intrusions along the northeastern margin of the Paleocene Ruby Range batholith into coeval volcanic rocks and associated hypabyssal intrusions of the Rhyolite Creek volcanoplutonic complex suggested high potential for porphyry and epithermal vein deposits (the "porphyry-to-epithermal transition") in that area. It is interesting to note that a slightly older (Late Cretaceous; ~78-75 Ma)

"porphyry-to-epithermal transition" occurs in exactly the same area, and is also known to be associated with porphyry and skarn mineralization.

Results of our study highlight the uncertainty that presently exists regarding the age and extent of Late Cretaceous and Paleocene magmatism in southwestern Yukon, and tectonic setting(s) in which the various magmatic events occurred and their mineral potential. More focused work is required to resolve this and to provide a more robust metallogenic framework for this highly prospective region.

ACKNOWLEDGMENTS

Fieldwork for this study as well as whole rock geochemistry and tracer isotope analysis was partially funded by a Lithoprobe University Supporting Geoscience grant to GM. GM acknowledges Rob Creaser (University of Alberta) for guidance and advice regarding the radiogenic isotope data. JM thanks the staff of the Pacific Centre for Isotopic and Geochemical Research (University of British Columbia) for assistance in the U-Pb analytical work. A critical review of the manuscript was provided by Don Murphy.

REFERENCES

Allan, M.M., Mortensen, J.K., Hart, C.J.R., Bailey, L.A., Sanchez, M.G., Ciolkiewicz, W., McKenzie, G.G., and Creaser, R.A., 2013. Magmatic and metallogenic framework of west-central Yukon and eastern Alaska. Society of Economic Geologists, Special Publication 17, p. 111–168.

Bacon, C.R., Bruggman, P.E., Christiansen, R.L., Clynne, M.A., Donnelly-Nolan, J.M., and Hildreth, W., 1997. Primitive magmas at five Cascade volcanic fields: Melts from hot heterogeneous sub-arc mantle. Canadian Mineralogist, vol. 35, p. 397-423.

Blumenthal, V.H., 2010. A geochemical study of the mineralization at the Hopper property, Yukon: A case study of an atypical copper occurrence. Unpublished MSc thesis, University of Waterloo, 119 p.

Cockfield, W.E., 1927. Aishihik Lake District, Yukon. Geological Survey of Canada, Summary Report, 1926, part A, p. 1-13.

Colpron, M., 2013. Yukon bedrock geology map (digital). <*http://ygsftp.gov.yk.ca/YGSIDS/compilations/Yukon_Geology_update_Nov2013.gdb.zip*>.

Erdmer, P. and Mortensen, J.K., 1993. A 1200 km long Eocene metamorphic-plutonic belt in the northwestern Cordillera: evidence from southwestern Yukon. Geology, vol. 21, p. 1039-1042.

Irvine, T.N., and Baragar, W.R.A., 1971. A guide to the chemical classification of the common volcanic rocks. Canadian Journal of Earth Sciences, vol. 8, p. 523-548.

Israel, S., Cobbett, R., Westberg, E., Stanley, B., and Hayward, N., 2011a. Preliminary bedrock geology of the Ruby Ranges, southwest Yukon (Parts of NTS 115G, 115H, 115A and 115B) (1:150 000-scale). Yukon Geological Survey, Open File 2011-2.

Israel, S., Murphy, D.C., Bennett, V., Mortensen, J.K., and Crowley, J., 2011b. New insights into the geology and mineral potential of the Coast Belt in southwestern Yukon. *In:* Yukon Exploration and Geology, K.E. MacFarlane, L.H. Weston, and C. Relf (eds.), Yukon Geological Survey, p. 101-123.

Israel, S. and Westberg, E., 2011. Preliminary geological map of the northwestern Aishihik Lake area, parts of NTS 115H/12 and 13 (1:50 000-scale). Yukon Geological Survey Open File 2011-31.

Israel, S. and Westberg, E., 2012. Geology and mineral potential of the northwestern Aishihik Lake map area, parts of NTS 115H/12 and 13. *In:* Yukon Exploration and Geology 2011, K.E. MacFarlane and P.J. Sack (eds.), Yukon Geological Survey, p. 103-113.

Johnson, D.M., Hooper P.R., and Conrey, R.M., 1999. XRF analysis of Rocks and Minerals for Major and Trace Elements on a single low dilution Li-tetraborate fused bead. Advances in X-ray Analysis, vol. l 41, p. 843-867.

Johnston, S.T., 1993. Geological evolution of Nisling Assemblage and Stikine Terrane in the Aishihik Lake area, southwest Yukon. Unpublished PhD thesis, University of Alberta, 336 p.

Johnston, S.T., Mortensen, J.K., and Erdmer, P., 1996. Igneous and meta-igneous age constraints for the Aishihik metamorphic suite, southwest Yukon. Canadian Journal of Earth Sciences, vol. 33, p. 1543-1555.

Johnston, S.T. and Timmerman, J.R., 1994. Geology of the Aishihik Lake and Hopkins Lake map areas (115H6/7), southwestern Yukon. *In:* Yukon Exploration and Geology 1993, S.R. Morison (ed.), Indian and Northern Affairs Canada, Exploration and Geological Services Division, p. 93-110.

Johnston, S.T. and Timmerman, J.R., 1997a. Geology of Aishihik Lake map area, Yukon (NTS 115 H/6). Exploration and Geological Services Division, Yukon, Indian and Northern Affairs Canada. Geoscience Map 1997-8.

Johnston, S.T. and Timmerman, J.R., 1997b. Geology map of the Hopkins Lake area, Yukon (115H/7) (1:50 000 scale). Exploration and Geological Services Division, Yukon, Indian and Northern Affairs Canada. Geoscience Map 1997-9.

Knaack, C.M., Cornelius, S., and Hooper, P.R. 1994. Trace element analysis of rocks and minerals by ICP–MS. Washington State University, Geology Department, Open File Report.

Le Bas, M.J., LeMaitre, R.W., Streckeisen, A., and Zanettin, B., 1986. A chemical classification of volcanic rocks based on the total alkali silica diagram. Journal of Petrology, vol. 27, p. 745-750.

Lewis, J., 1997. Geology, alteration, and mineralization of the Sato copper porphyry property, southwestern Yukon Territory, Canada. Unpublished directed study report for J.K. Mortensen, 68 p.

Lewis, J. and Mortensen, J.K., 1998. Geology, alteration, and mineralization of the Sato porphyry copper prospect, southwestern Yukon. *In:* Yukon Exploration and Geology 1997, Roots, C.F. (ed.), Indian & Northern Affairs Canada/Department of Indian & Northern Development: Exploration & Geological Services Division, p. 153-160.

Miskovic, A. and Francis. D., 2004. The Early Tertiary Sifton Range volcanic complex, southwestern Yukon. *In:* Yukon Exploration and Geology 2003, D.S. Edmond and L.L. Lewis (eds.), Yukon Geological Survey, p. 143-155.

Morris G.A. and Creaser, R.A., 1998. Petrogenesis of the Eocene Mt. Skukum and Bennett Lake igneous complexes, southwest Yukon Territory, Canada. Abstracts with Programs, Geological Society of America, vol. 30, p. 55-56.

Morris G.A. and Creaser R.A., 2003. Crustal recycling during subduction at the Eocene Cordilleran margin of North America: a petrogenetic study from the southwestern Yukon. Canadian Journal of Earth Sciences, vol. 40, p. 1805-1821.

Mortensen J.K., Hall, B.V., Bissig, T., Freidman R.M., Danielson, T., Oliver, J., Rhys, D.A., Ross, K.V., and Gabites, J.E., 2008. Age and paleotectonic setting of massive sulphide deposits in the Guerrero terrane of central Mexico: Constraints from U-Pb Age and Pb isotope studies. Economic Geology, vol. 103, p. 117-140.

Murphy, D.C. 2007. The three "Windy KcKinley" terranes of Stevenson Ridge (115jk), western Yukon. *In:* Yukon Exploration and Geology 2006, D.S. Emond, L.L. Lewis, and L.H. Weston (eds.), Yukon Geological Survey, p. 223-236.

Peacock, M.A., 1931. Classification of igneous rock series. Journal of Geology, vol. 39, p. 54-67.

Pearce, J.A., 1996. A user's guide to basalt discrimination diagrams. *In:* Trace element geochemistry of volcanic rocks; applications for massive sulphide exploration, A.H. Bailes, E.H. Christiansen, A.G. Galley, G.A. Jenner, J.D. Keith, R. Kerrich, D.R. Lentz, C.M. Lesher, S.B. Lucas, J.N. Ludden, J.A. Pearce, S.A. Peloquin, R.A. Stern, W.E. Stone, E.C. Syme, H.S. Swinden, and D.A. Wyman (eds.), Short Course Notes, Geological Association of Canada, vol. 12, p. 79-113.

Pearce, J.A., Harris, B.W., and Tindle, A.G., 1984. Trace element discrimination diagrams for the tectonic interpretation of granitic rocks. Journal of Petrology, vol. 25, p. 956-983.

Peccerillo, A. and Taylor, S.R., 1976. Geochemistry of Eocene calc-alkaline volcanic rocks from the Kastamonu area, Northern Turkey. Contributions to Mineralogy and Petrology, vol. 58, p. 63-81.

Sun S., and McDonough, W.F., 1989. Chemical and isotopic systematics of oceanic basalts: implications for mantle composition and processes. *In:* Magmatism in the Ocean Basins, A.D. Saunders and M.J. Norry (eds.), Geological Society Special Publication, no. 42, p. 313-345.

Tempelman-Kluit, D.J., 1974. Reconnaissance geology of the Aishihik Lake, Snag and part of the Stewart River map areas, west-central Yukon (115A, 115F, 115G and 115K). Geological Survey of Canada Paper 73-41, 97 p.

Winchester, J.A. and Floyd, P.A., 1977. Geochemical discrimination of different magma series and their differentiation products using immobile elements. Chemical Geology, vol. 20, p. 325-343.

Yukon MINFILE, 2013. Yukon MINFILE - A database of mineral occurrences. Yukon Geological Survey, <*http://data.geology.gov.yk.ca*> [accessed November 1, 2013].